Structural Optimization of Highly Branched Thermally Responsive Polymers as a Means of Controlling Transition Temperature

Kai Chang, Nathan C. Rubright, Patti D. Lowery, Lakeshia J. Taite

School of Chemical & Biomolecular Engineering, Georgia Institute of Technology, 311 Ferst Dr. NW, Atlanta, Georgia 30332-0100
Correspondence to: L. J. Taite (E-mail: lakeshia.taite@chbe.gatech.edu)

Received 2 October 2012; accepted 19 January 2013; published online 14 February 2013
DOI: 10.1002/pola.26596

ABSTRACT: Highly branched "smart" polymers have emerged as a unique class of polymers with wide-ranging applications. Poly(N-isopropylacrylamide) (pNIPAAm) is at the forefront of stimuli-responsive polymers; however, few transition temperature-modification methods of linear pNIPAAm have been explored in highly branched systems. In this study, the three primary techniques of transition temperature modification of linear pNIPAAm are investigated for their efficacy on highly branched polymers. Of these techniques, cosolvent-mediated tacticity control demonstrates an effect opposite of that which is expected. Temperature transition control via end-group modification shows a marked decrease in efficacy in highly branched systems, despite highly branched systems having more end groups per polymer. Copolymerization with hydrophilic comonomers exhibits varying changes in efficacy compared to linear analogs, lending insights into the specific effects on the structured water surrounding the copolymer. While copolymerization proved to be most versatile in changing the transition temperature, all of the techniques showed interesting secondary effects. © 2013 Wiley Periodicals, Inc. J. Polym. Sci., Part A: Polym. Chem. **2013**, *51*, 2068–2078

KEYWORDS: branched; copolymerization; degree of branching; LCST; reversible addition fragmentation chain transfer (RAFT); poly(*N*-isopropylacrylamide); tacticity; thermal properties

INTRODUCTION Polymer architecture has been the subject of much research in recent years. From star polymers to dendrimer-like polymers, architecture has played a crucial role in developing new properties in polymeric materials.[1–4] This has been especially true for stimuli-responsive polymers such as the thermally responsive poly(*N*-isopropylacrylamide) (pNIPAAm), where modifications in the architecture have opened up new possibilities in bioprocesses.[5–7] pNIPAAm has long been studied as a "smart" biomaterial due to its bioinert and thermally responsive characteristics. Changing the architecture to highly branched pNIPAAm continues the trend of using topology to modify properties. The resulting polymer exhibits a globular structure that can be exploited for controlled drug delivery, a subject of much current research.[8–10] In addition to its globular structure, highly branched pNIPAAm also undergoes a thermal transition from hydrophilic to hydrophobic on reaching a critical temperature and can be used as a system to control drug delivery based on local temperature. This provides the basis of a controlled release drug delivery system, which can provide clinicians with the ability to control when drugs are delivered, and therefore better monitor their patients' dosages. This ability, along with the potential of targeting these delivery systems, may prove especially important in the realm of chemotherapy for cancer treatment, establishing a means to limit the harsh side effects of chemotherapeutic drugs.[8] Because of the sensitivity of such a system, deviations in transition temperature of even a few degrees can lead to significant failure. Therefore, understanding the effects of branching on this type of system can not only lead to optimally designed drug delivery constructs but also provide insights into the variety of controls that need to be in place to successfully modify responsive highly branched polymer systems.

Highly branched polymers can be synthesized by a process, similar to convergent dendrimer synthesis, which utilizes a branching agent to converge towards a central moiety.[3,11] Such architecture provides a dense surface and a relatively sparse interior with ample space to encapsulate drugs, while bypassing many of the challenges posed by traditional dendrimer synthesis. The basic scheme for highly branched polymer synthesis is a one-pot condensation or polymerization in which branching moieties are present.[3,11–13] By condensing the branching units, a three-dimensional globular structure, not unlike that of a dendrimer, can be achieved.

The controlled synthesis of a stimuli-responsive highly branched polymer system is not trivial. There are three key

Additional Supporting Information may be found in the online version of this article.

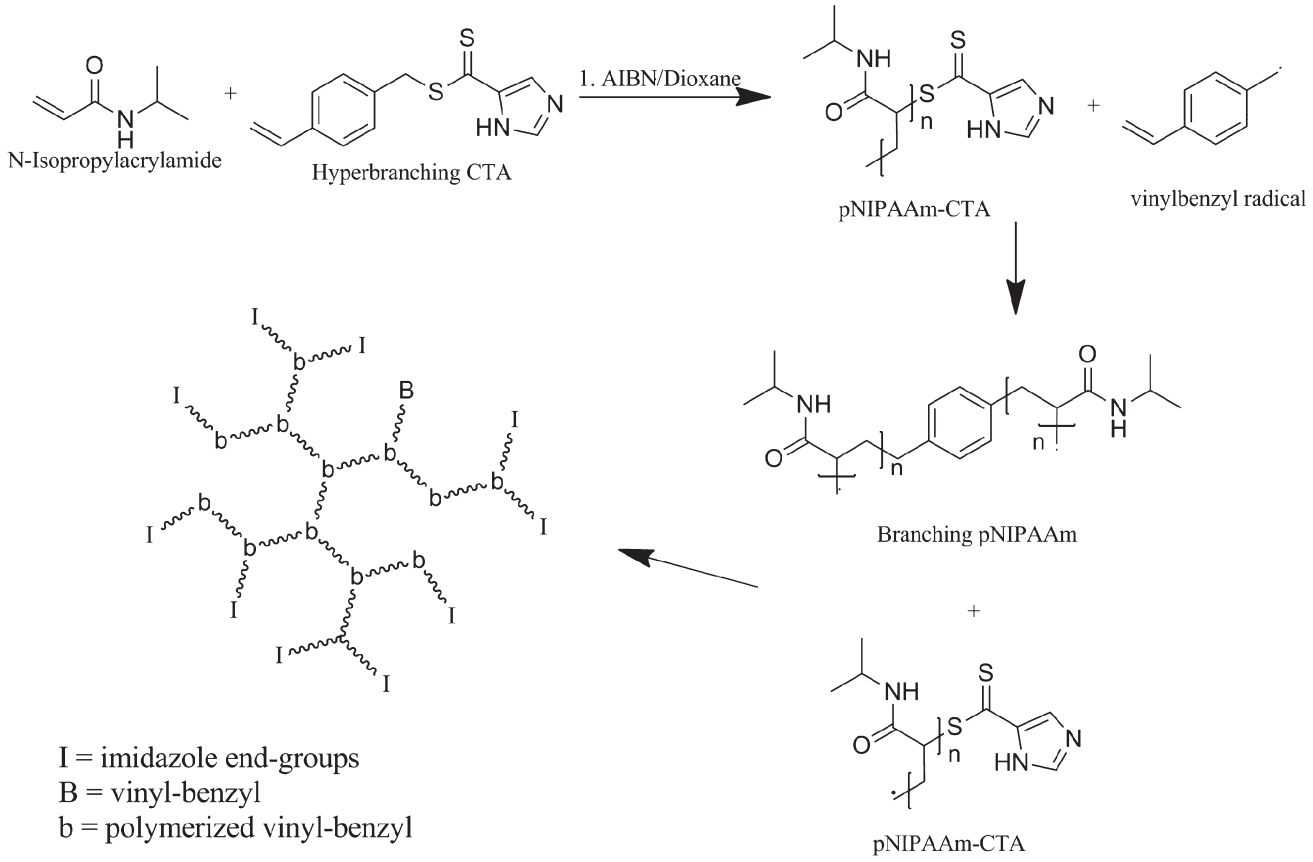

SCHEME 1 Highly branched RAFT polymerization using 4-vinylbenzylimidazoledithioate as a chain transfer agent.

issues when synthesizing such a polymer: control over the polymer molecular weight distribution, branching, and effects on the response mechanism, which in this case is the lower critical solution temperature (LCST), represented by the cloud point temperature (T_{cp}). Molecular weight control of highly branched polymers has been attempted through various polymerization schemes such as atom transfer radical polymerization[14,15] and reversible addition fragmentation chain transfer (RAFT) polymerization[7,16,17] to varying degrees of success. Mathematical models of such polymerization schemes conclude that such systems can produce macromolecules of low polydispersity indices (PDIs) of around 1.1, with individual branch segments having PDIs of less than 1.4;[18] however, PDIs greater than 2.0 are commonly observed in such systems.[13,14] Controlling the degree of branching (DB) has been attempted through careful monomer selection and reaction condition control[11,19,20] as well as the use of different polymerization schemes;[11,21] however, these attempts are primarily focused on the hyperbranching of AB_x type monomers and not the branching of long polymer chains in a dendrimer-like structure. The effects of branching on the stimulus response of "smart" polymers are an important consideration because the change in polymer topology can have a significant impact on the magnitude of the response. For example, highly branched pNIPAAm shows a significant decrease in the T_{cp} compared to its linear counterpart (~2–5 °C).[17,22]

In this work, polymerization was conducted using RAFT polymerization, a form of controlled free radical polymerization.[23] The RAFT scheme controls polymerization by introducing a chain transfer agent (CTA), usually a di- or trithiocarbonate, that reversibly reacts with polymerizing chains to form a dynamic equilibrium between active and dormant chains. This causes a significant decrease in termination reactions, and subsequently the PDI of the final polymers.

Branching of pNIPAAm was induced using a branching CTA during RAFT polymerization. 4-Vinylbenzylimidazoledithioate has previously been well characterized as a branch-inducing RAFT agent[13] and the vinyl group attached to the CTA makes it is possible to induce polymerization along two directions concurrently (Scheme 1). This secondary direction of polymerization induces the branching effect.[12,16,17]

In this study, we explore three different techniques employed in LCST manipulation; tacticity control, end-group control, and copolymerization, and investigate their utility and limitations in the highly branched architecture. Incorporation of tacticity control into polymerization schemes for highly branched polymers through solvent interactions introduces new areas of complexity, and to the best of our knowledge, such control has not previously been explored. End-group effects on the transition properties of highly branched pNIPAAm are also largely unknown. Because of the effects

exhibited by the end groups on linear pNIPAAm,[24] it is expected that this form of T_{cp} control is even more effective for highly branched pNIPAAm because there are more end groups available for highly branched polymers. While copolymerization of pNIPAAm with various comonomers in highly branched systems has been briefly explored,[12,17] comparisons to linear models have not been done. By exploring these three models of LCST control on highly branched pNIPAAm, we demonstrate that these methods not only have different efficiency in controlling the LCST, but can also have unexpected effects on the polymer product.

EXPERIMENTAL

Materials

N-Isopropylacrylamide was purchased from TCI America and recrystallized in 9:1 hexanes:benzene. 4(5)-Imidazole dithiocarboxylic acid, cesium carbonate, dimethyl acrylamide (DMA), acrylamide (AAm), acrylic acid (AAc), 1-hexylamine, 5,5′-dithiobis(2-nitrobenzoic acid), tributylphosphine, 1, 4 dioxane, 3-methyl-3-pentanol (3Me3PenOH) were purchased from Sigma Aldrich and used without further purification.

4-Vinylbenzylimidazoledithioate (1) Synthesis

Synthesis of **1** was modified from the procedure set forth by Carter et al.[12] Briefly, 2.2 g of 4(5)-imidazole dithiocarboxylic acid and 15.4 g of cesium carbonate were dissolved in 45 mL of dimethylformamide. The solution was purged with nitrogen and stirred for 30 min. 4-Vinylbenzyl chloride (1.69 mL) was added to the reaction vessel and was reacted for 70 h. The raw product was then filtered to remove excess cesium carbonate. The filtrate was diluted with 500 mL of nanopure water and extracted with 200 mL of dichloromethane twice. The DCM mixture was subsequently concentrated using a rotary evaporator to reduce the volume to ~50 mL. The mixture was then passed through a silica column with 2.5% methanol in DCM and then again through an alumina column with 2% methanol in DCM. The appropriate fraction was collected and the resulting product was dried, yielding bright orange crystalline product. The product **1** was confirmed (see Supporting Information) using ^{1}H NMR (400 MHz, $CDCl_3$, δ): 7.8 (d, 2H); 7.3 (d, 2H); 6.6 (q, 1H); 5.6 (d, 1H); 5.15 (d, 1H); 4.5 (s, 1H).

Tacticity Control

Polymerization of NIPAAm was carried out with **1** in the presence and absence of 3Me3PenOH to control tacticity. Two ratios of 3Me3PenOH were tested: 4:1 and 10:1 of 3Me3PenOH:NIPAAm. For example, under the 4:1 condition, a 1.03 g mixture of 100:1:0.5 ratio of NIPAAm:**1**:AIBN and 4 mL of 3Me3PenOH was placed in a sealed 25-mL round-bottom flask equipped with a magnetic stir bar. The mixture was purged with nitrogen for 15 min and 10 mL of nitrogen-purged 1, 4 dioxane was added. The solution was reacted at 65 °C for 48 h and was quenched by exposure to air. The pNIPAAm was precipitated into diethyl ether and collected via filtration. The pNIPAAm was then dissolved in nanopure water, and dialyzed with a 2000 MWCO membrane dialysis cassette. During dialysis, the water was changed every hour for the first 4 h and then allowed to proceed overnight. The samples were then frozen and lyophilized.

End-Group Modification

pNIPAAm was synthesized similarly to the methods described above. For instance, a 10.3 g mixture of 100:1:0.5 ratio of NIPAAm:**1**:AIBN was placed in a sealed 25-mL round-bottom flask equipped with a magnetic stir bar. The mixture was purged with nitrogen for 15 min and 10 mL of nitrogen-purged 1,4 dioxane was added. The solution was reacted at 65 °C for 48 h and was quenched by exposure to air. The pNIPAAm was precipitated into diethyl ether and collected via filtration. The pNIPAAm was then dissolved in nanopure water, and dialyzed as previously described with a 2000 MWCO membrane dialysis cassette. The sample was then frozen and lyophilized.

The freeze-dried pNIPAAm was then was then subjected to aminolysis using hexylamine. Thiol functionality was maintained using tributylphosphine. Briefly, 1 g of pNIPAAm was reacted with 660 μL of 1-hexylamine and 247 μL of tributylphosphine in 25 mL of 1, 4 dioxane under nitrogen for 2 h. The product was precipitated in cold ether, filtered, and dried *in vacuo*. An Ellman's assay was conducted to confirm the presence of thiols.[25] In brief, 100 μL of 100 μM solution of lysed pNIPAAm in 0.1 M Tris buffer, pH 8 was reacted with 100 μL of 4 mg/mL of 5,5′-dithiobis(2-nitrobenzoic acid) in Tris buffer. Absorbance was measured at 410 nm on a Beckman DTX 880 Multimode Plate Reader and was compared to standards made with known concentrations of L-cysteine.

End groups were introduced using thiol-Michael addition. A 1:1.2 ratio of thiols to -enes were conjugated using 1-hexylamine as the base. In a typical reaction, 300 mg of cleaved pNIPAAm was dissolved in 5 mL of Tetrahydrofuran (THF) and 60 μL of DMA or 40 μL of AAc was added along with 50 μL of 1-hexylamine. The solutions were reacted at 40 °C overnight and dried in a vacuum oven. They were then redissolved in nanopure water, dialyzed as previously described using 2000 MWCO dialysis cassettes, and lyophilized. Conjugation was confirmed using gel permeation chromatography (GPC) and ^{1}H NMR (see Supporting Information).

Random Copolymer Synthesis

Copolymerization of NIPAAm was carried out with **1**. Copolymers of pNIPAAm with DMA, acrylamide (AAm), and AAc were synthesized with varying amounts of comonomer. For example, a 1.03 g mixture of 90:10:1:0.5 ratio of NIPAAm:AAc:**1**:AIBN was placed in a sealed 25-mL round-bottom flask equipped with a magnetic stir bar. The mixture was purged with nitrogen for 15 min and 10 mL of nitrogen-purged 1, 4 dioxane was added. The solution was reacted at 65 °C for 48 h and was quenched by exposure to air. The copolymers were precipitated in diethyl ether and collected via filtration. Successful copolymerization was confirmed using proton NMR.

TABLE 1 pNIPAAm Synthesized with Various Amounts of 3Me3PenOH

3Me3PenOH to Monomer Ratio	M_n[a]	M_w[a]	PDI[a]	DB[b]	ANB[b]
0	12,800	22,500	1.8	0.30	0.09
4:1	14,200	25,300	1.8	0.26	0.09
10:1	14,700	26,000	1.8	0.26	0.09

[a] M_n, M_w, and PDI were calculated via GPC using polystyrene standards.
[b] Degree of branching (DB) and average number of branches (ANB) were obtained via NMR using eqs 1 and 2.

Characterization

Characterization was performed using GPC, NMR, matrix-assisted laser desorption ionization (MALDI) mass spectrometry, and UV–visible spectrometry. GPC was conducted on a GPC-50 Plus (Agilent) equipped with two PLgel 3-μm MIXED-E columns with UV, RI, and viscosity detectors. THF was used as the polymer solvent and eluent. A flow rate of 1 mL/min was used. Chromatograms were compared with those of polystyrene standards (Agilent). ^{1}H NMR was conducted on a Varian Mercury Vx 400 spectrometer using chloroform-*d* as a solvent. High-temperature ^{1}H NMR (150 °C) was conducted on a Bruker DMX 400 spectrometer using dimethylsulfoxide d_6 as solvent. Mass spectrometry was run on an Applied Biosystems 4700 Proteomics Analyzer with a 200-Hz Nd:YAG laser using CHCA matrix and reflecting detector. Turbidity was measured using UV–vis spectrometry conducted at constant pH (7.0 ± 0.1) using a Cary 50 UV–vis spectrophotometer (Agilent) with a single-cell Peltier-thermostatted cell holder and accessory for temperature control. Scans were conducted every 0.1 °C, and the temperature was ramped at 1 °C/min.

RESULTS AND DISCUSSION

Effects of Using a Bulky Alcohol Cosolvent

In the past few years, several publications have discussed the use of stereocontrol as a method of modifying LCST.[26–29] According to Hirano et al., pNIPAAm polymers that are predominately syndiotactic have higher LCSTs than atactic pNIPAAm.[28] Similarly, isotactic pNIPAAm has a lower LCST than atactic pNIPAAm. Not only does the transition temperature change, but the profile also changes, with syndiotactic pNIPAAm having sharper transitions than atactic pNIPAAm.[28] Lewis acids and bulky alcohols in particular have been used to induce majority isotactic or majority syndiotactic poly (acrylamides).[28,30] 3Me3PenOH has been shown to be a particularly effective racemo diad-inducing agent, increasing the racemo diad content to up to 70% in linear systems, while being a more mild additive than similar Lewis bases.[28,31]

To explore the feasibility of using solvent-mediated tacticity control as a LCST-modifying agent, highly branched pNIPAAm was synthesized using a branching RAFT agent as seen in Scheme 1. The polymers displayed a slight orange tint, a residual effect from the orange coloration of the RAFT agent used in the polymerization. Branching was confirmed via GPC, with the polymers exhibiting Mark-Houwink α values on the order of 0.13, which is well within the realm of highly branched pNIPAAm (see Supporting Information).[13] Three ratios of 3Me3PenOH were used in this study. The polymer weights and PDIs are shown in Table 1 and the GPC chromatograms are shown in Figure 1. The molecular weight trend indicates that even under the same polymerization conditions (65 °C, 48 h), the polymers form larger highly branched structures compared to the control reaction that did not contain the bulky alcohol. This increase in molecular weight is likely due to increased branching and is supported by the branching data.

The DB and average number of branches (ANB), a measure of branching density, were calculated using ^{1}H NMR using the equations put forth by Frechet et al. (eq 1)[3] and Frey et al. (eq 2):[32]

$$DB = \frac{D + T}{D + T + L} \quad (1)$$

$$ANB = \frac{D}{D + L} \quad (2)$$

T, *D*, and *L* represent terminal, dendritic, and linear groups, respectively. DB and ANB are commonly used to describe the branching properties of highly branched polymers.[17,19,33–35] ANB was calculated to be the ANB per nonterminal, nonlinear unit and the results of both parameters are shown in Table 1.[32]

The DB values decreased with increasing amounts of 3Me3PenOH; however, the branching density remained constant. This provides several insights into the polymer characteristics. First, the average linear segment length remains unchanged due to the constant ANB. This means that the overall change in size is not due to individual segments becoming longer during the polymerization. Second, the

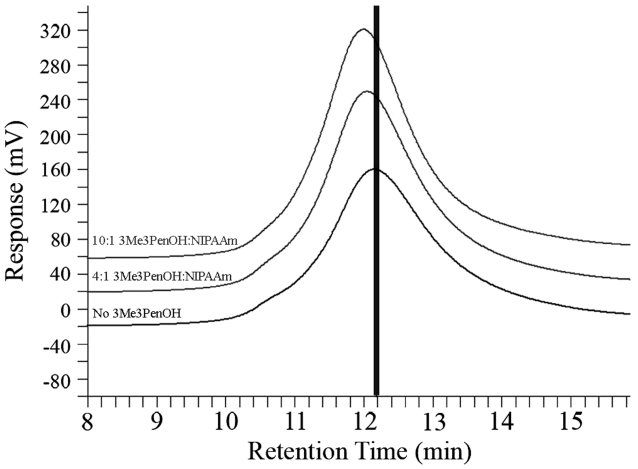

FIGURE 1 GPC traces showing the molecular weight as the amount of 3Me3PenOH increases. The vertical line indicates retention time of the main polymer peak synthesized without 3Me3PenOH. The molecular weight increases significantly with increasing 3Me3PenOH.

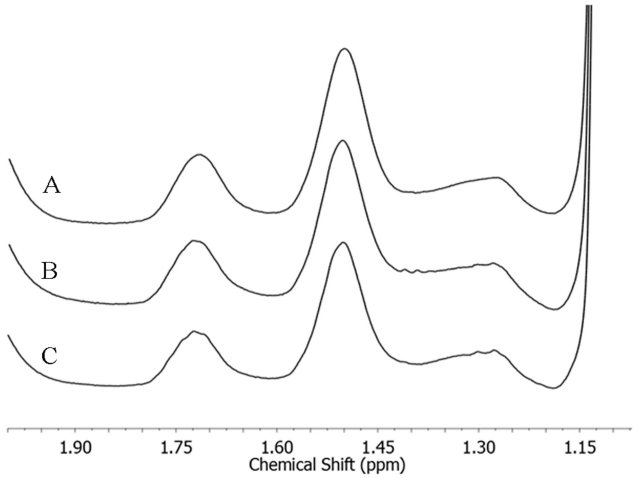

FIGURE 2 ^{1}H NMR spectra of methine backbone peaks conducted at 150 °C. (A) 10:1 3Me3PenOH:NIPAAm showed 52% racemo diads, (B) 4:1 3Me3PenOH:NIPAAm showed 55% racemo diads, (C) control pNIPAAm showed 56% racemo diads. Racemo diads are indicated by the peak at 1.50 ppm while meso diads are indicated at 1.28 and 1.73 ppm.

proportion of linear chains in the overall polymer is increasing. This is consistent with increased polymer size. Taken together, the data clearly indicates that the increased size of the polymer is due to more branches per polymer. Statistically, the segments remain at ~10 linear units per branch unit but the number of branches increases with the solvent ratio.

The increase in the number of branches, combined with the constant polymer PDI, paints an interesting picture of the state of the polymer. Despite having more branches and therefore more chances of variability, the polymer does not become more polydisperse.

Characterization of Tacticity Effects

The tacticity of the polymers were confirmed using high-temperature ^{1}H NMR spectrometry, as shown in Figure 2. Interestingly, the amount of racemo diads decreased from 56% in the control to 52% in the polymer with a 10:1 ratio of 3Me3PenOH:NIPAAm. This change in racemo diad content is contrary to that of linear polymers run under similar conditions which show an increased racemo diad content of 61%.[24] While this initially seems counterintuitive for this system, considering the molecular weight effects observed in the polymer through the use of this cosolvent, it may be a confirmation of accelerated polymerization induced by 3Me3PenOH, a process known to occur during radical polymerization in polar protic solvents.[24,28,36] The accelerated polymerization reduces any preferential backbone configuration.

Racemo diad formation using bulky alcohols is caused by hydrogen bonding between the alcohols and the acrylamide group, which sterically hinders polymerization in the meso diad form.[37] As proper hydrogen bonding for this effect is temperature dependent, preferring low temperatures, racemo diad formation was already weak at the polymerization temperature. Lower temperature polymerizations, including a reaction initiated at high temperature for 1 h before continuation at room temperature and UV-initiated room temperature polymerization, were attempted. However, despite successful polymerization in the absence of the RAFT agent, these attempts failed in the scheme of interest due to the reaction kinetics of the RAFT agent used. At the normal polymerization temperature, any nominal racemo diad preference may have been quenched by the acceleration effect of the cosolvent, because the increased reaction rate favored atactic polymerization. As this effect was not seen in the linear counterpart,[24] even at high polymerization temperatures, it can therefore be attributed to the branching architecture of the polymer and a factor in its polymerization.

UV–vis spectroscopy was used to assess the T_{cp} of highly branched pNIPAAm, as seen in Figure 3(A). T_{cp} is defined as the point where the transmittance drops to 50% of the

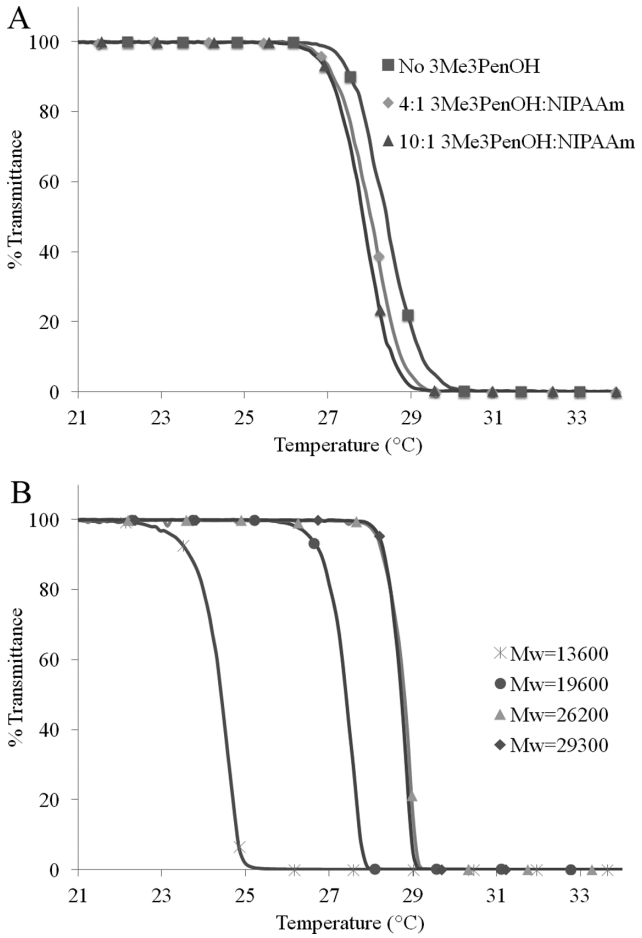

FIGURE 3 Turbidity measurements with readings taken every 0.1 °C. (A) T_{cp} of pNIPAAm with varying amounts of 3Me3PenOH as cosolvent. T_{cp} decreases with increasing 3Me3PenOH content. (B) T_{cp} of pNIPAAm of varying molecular weights without the use of 3Me3PenOH. T_{cp} increases with increasing molecular weight.

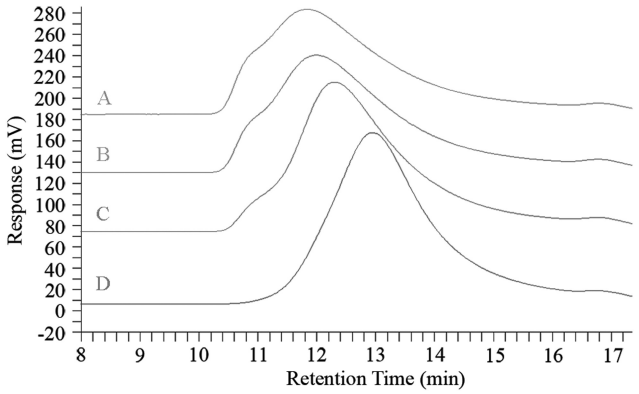

FIGURE 4 GPC traces of different molecular weight hyperbranched pNIPAAm synthesized without 3Me3PenOH. From top to bottom, the weight average molecular weights were 29,300 (A), 26,200 (B), 19,600 (C), and 13,600 (D), respectively. The PDIs were 1.7, 1.8, 1.9, and 1.8, respectively.

initial value. The results are consistent with the observed increase in meso diad content. It is well known that increasing the racemo diad content of linear pNIPAAm increases the T_{cp}, while increasing the meso diad content decreases the T_{cp}.[38] In this case, the T_{cp} decreased from 28.4 °C without 3Me3PenOH to 28.0 °C with a 4:1 ratio of 3Me3PenOH:NIPAAm to 27.9 °C with a 10:1 ratio of 3Me3PenOH:NIPAAm. These differences, while small, are statistically significant as assessed by an ANOVA test with Tuckey's post-hoc analysis ($n = 3$, $P < 0.05$). They are also consistent with theory and suggest that with stronger tacticity controls, significant changes in the T_{cp} may be achieved.

As a matter of comparison, similar molecular weights of highly branched pNIPAAm were prepared using differing molar ratios of monomer to RAFT agent as the controlling factor for the molecular weight, and the opposite relation between molecular weight and T_{cp} was observed. As seen in Figure 3(B), in the absence of 3Me3PenOH, increasing molecular weight increases the T_{cp}. This is due to the increased aggregation caused by the polymerization process. The high molecular weight shoulder increases in intensity as degree of polymerization and molecular weight increase, indicating a more bimodal distribution with a significant number of higher molecular weight particles, as seen in Figure 4.

End-Group Control

Previous studies have shown that end groups have significant effects on the transition temperature of linear pNIPAAm.[24,39] In our system, the RAFT groups double as the chain ends in our branching scheme and can be easily cleaved via aminolysis.[33,40] The remaining thiols can then be modified through thiol-Michael addition chemistry.[41–43]

Because of the increased number of end groups in a highly branched polymer, it is expected that the end groups will play an even greater effect on these polymers. To test this, the RAFT agent was cleaved to leave a thiol, and thiol-Michael addition chemistry was used to attach two different hydrophilic end groups, DMA and AAc, as shown in Scheme 2.

In the initial cleavage of the polymer, the molecular weight decreased from $M_w = 30{,}000$ g/mol to $M_w = 25{,}800$ g/mol. This indicates a removal of ~37 1-imidazole-5-carbothialdehyde groups per polymer. The removal of these slightly hydrophilic end groups does change the T_{cp} slightly as seen in Figure 5, but the 0.3 °C difference is small compared to the changes observed in linear pNIPAAm.[24,39,44]

On inclusion of AAc and DMA end groups the M_w increased to 29,300 g/mol, indicating >90% conjugation. ^{1}H NMR analysis further confirmed 7.5% end-group content in the AAc system and 10% end-group content for the DMA system (see Supporting Information). The combination of the MW and NMR data indicates between 7 and 12 repeat units per end group, which is comparable to linear systems of 900–1400 g/mol with one modified end group. Previous discussions on the effect of end groups on linear pNIPAAm systems show increases in transition temperature of more than 5 °C, even at molecular weights of >10,000 g/mol for amine- and ether-terminated polymers.[39] As seen in Figure 5, incorporating DMA end groups only increased the T_{cp} by 0.5 °C while incorporating AAc end groups increased the T_{cp} by 1.2 °C. This discrepancy suggests that the branching architecture interferes with the efficacy of the end groups as LCST-modifying agents. Recent studies on the segmental mobility of various pNIPAAm end groups suggest a correlation between the two; with hydrophobic end groups exhibiting limited segmental mobility and hydrophilic end groups exhibiting enhanced segmental mobility.[45] The short chains of 8–10 repeat units between branching segments naturally inhibit segmental mobility in highly branched pNIPAAm, thereby limiting the effects of the hydrophilic end groups attached to these polymers.[46] The data therefore suggests that a decrease in end group mobility may strongly affect the ability of the end group to change the LCST of the polymer. In fact, the lack of mobility makes highly branched polymers extremely resistant to end-group-based LCST modification despite the large number of end groups and the small, adjusted equivalent linear size.

Even with the small overall change in LCST, the larger of the increases was caused by AAc end groups and is consistent with the literature.[47] In addition, both end groups increased the T_{cp} beyond the uncleaved state. This indicates that the degree of hydrophilicity does have an effect on the transition properties of highly branched pNIPAAm, although much diminished compared to linear systems.

Copolymerization

As the inclusion of tacticity control decreased the LCST and end-group control had a minimal effect on the LCST, the traditional method of copolymerization with hydrophilic monomers is the most promising method to induce the large LCST increase necessary for sufficiently high transition temperatures. To quantify the effectiveness of this method, three different common pNIPAAm copolymers were synthesized. The three different highly branched copolymers, pNIPAAm-*co*-DMA,

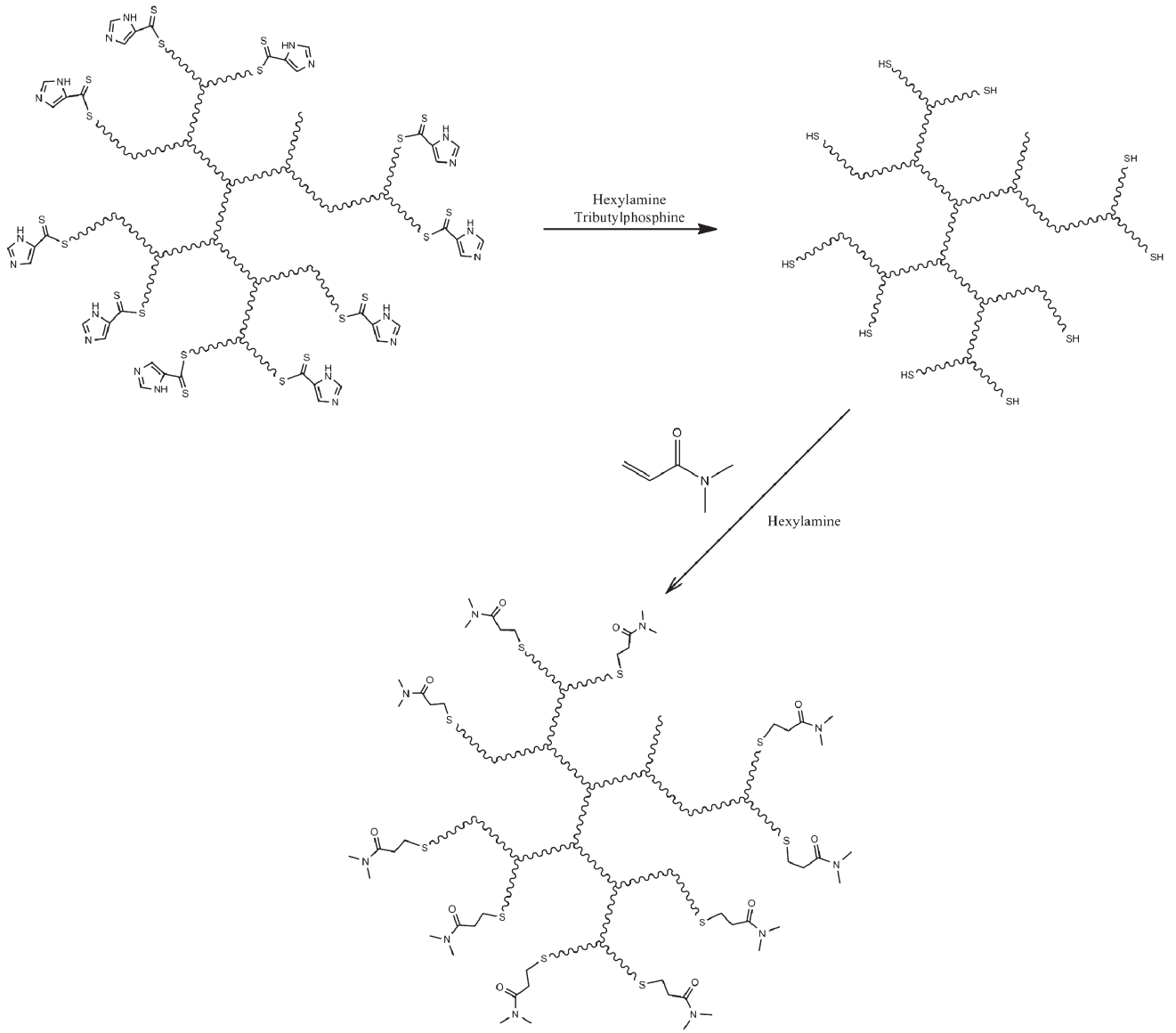

SCHEME 2 DMA end-group attachment to hyperbranched pNIPAAm. RAFT imidazole dithioate end groups were cleaved via aminolysis using hexylamine, generating thiol end groups. DMA was clicked onto the thiol end groups via thiol-Michael addition.

pNIPAAm-*co*-AAm, and pNIPAAm-*co*-AAc, show drastically different temperature transition profiles from a highly branched homopolymer of pNIPAAm. As seen in Figure 6, even with a constant 10% copolymer content, the effects on the final polymer exhibited varied dramatically.

A closer study of the effects of varying percentages of each copolymer on the overall transition temperature further reveals the differences between these systems. As seen in Figure 7, the -*co*-DMA system requires a large amount of copolymer to significantly change the transition temperature; a shift of 13.5 °C requires a copolymer content of 35%. Despite needing a large copolymer percentage to effect significant T_{cp} change, the transitions are relatively sharp, even at high copolymer content, with a transition range of 4.3 °C even at 50% copolymer content.

Similarly, as seen in Figure 8, the -*co*-AAm system also requires a large copolymer content to effect significant T_{cp} change, with a 19.3 °C increase requiring 30% copolymer content. While AAm is a more efficient copolymer than DMA for modifying the T_{cp}, it also increases the transition range to a greater degree, with 60% AAm showing a transition range of 10.8 °C.

Compared to the other two copolymers, the -*co*-AAc system is drastically more effective at changing the T_{cp}, as seen in Figure 9. A mere 5% copolymer content raises the T_{cp} by 11.6 °C. This efficacy is coupled with a dramatic broadening of the transition, with 15% AAc requiring more than a 30 °C range to fully transition.

The effect of hydrophilic and charged copolymers on the LCST of pNIPAAm has previously been explored in linear

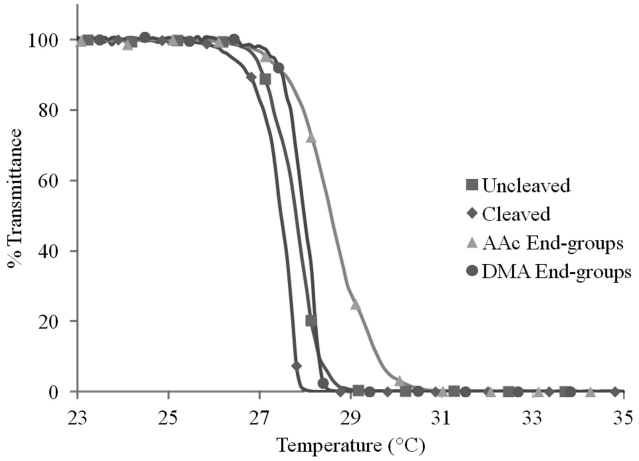

FIGURE 5 T_{cp} of highly branched pNIPAAm with various end groups. The uncleaved pNIPAAm shows a T_{cp} of 27.8 °C while the cleaved pNIPAAm shows a T_{cp} of 27.4 °C. The AAc end groups increased the T_{cp} to 28.6 °C while the DMA end groups increased the T_{cp} to 28.0 °C.

systems and concluded to be a result of fewer hydrophobic groups and greater polymer–water interactions.[47] While this is likely still true for highly branched polymers, the branched architecture enforces closer packing of polymer chain segments and reduces their degrees of freedom, yielding lower transition temperatures. When compared to a linear system, as seen in Figure 10(A), the branched architecture for *-co*-AAc demonstrates greater deviations as related to copolymer content. This indicates that in closer proximity, the additional AAc groups in highly branched systems are more effective at stabilizing hydrophilic interactions with structured water and disrupting hydrophobic interactions than in linear systems. The opposite effect is seen

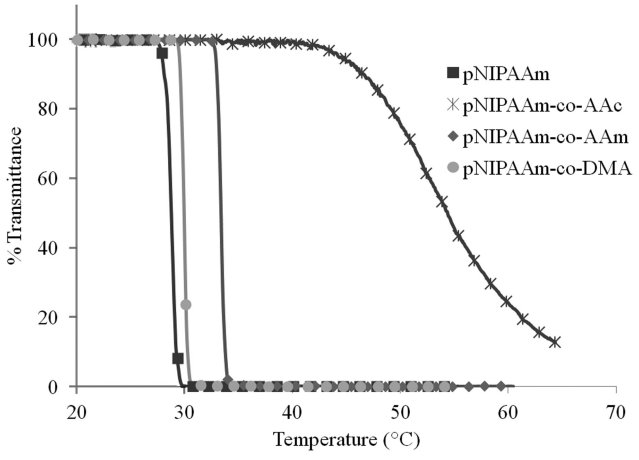

FIGURE 6 Temperature transition profiles for different copolymers. All copolymers contained 10% copolymer content. Highly branched pNIPAAm exhibited a sharp transition at 28.8 °C. AAc exhibited a broad transition at 54 °C. AAm and DMA exhibited sharp transitions at 33.4 and 29.9 °C, respectively.

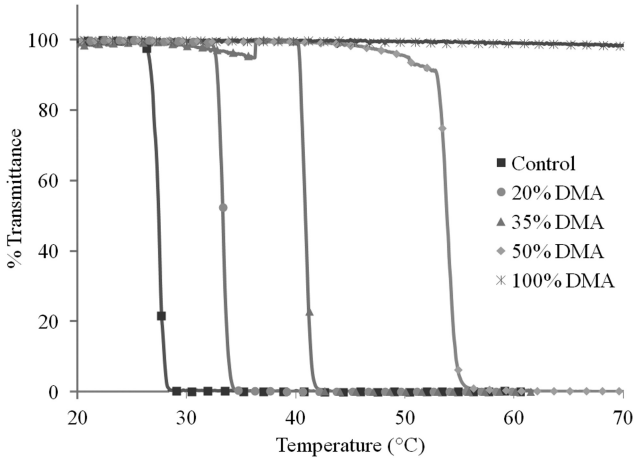

FIGURE 7 pNIPAAm-*co*-DMA copolymers and their T_{cp}s. Transitions were narrow and occurred at 33.3, 40.9, and 53.9 °C for 20, 35, and 50% copolymer content, respectively.

in Figure 10(B), with the linear DMA system being more effective at raising the LCST. This is due to the DMA having a similar hydrophilic/hydrophobic imprint as pNIPAAm, with hydrophobic dimethyl groups protruding from the hydrophilic acrylamide fragment. The reduced degrees of freedom and close packing of the highly branched system therefore encourages hydrophobic interactions with these chains and reduces the effectiveness of DMA as an LCST-modifying agent.

In addition to raising the LCST, clearly copolymer content has a broadening effect on the polymer transition, as seen in Table 2. The most effective system, *-co*-AAc, also exhibits the broadest transitions, while the least effective system, *-co*-DMA, has the sharpest transitions regardless of whether the copolymers are compared at the same copolymer content or at the same transition temperature. Furthermore, regardless of copolymer, transition ranges

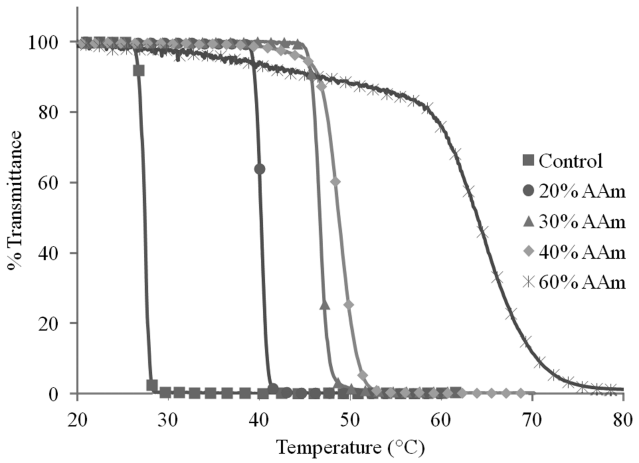

FIGURE 8 pNIPAAm-*co*-AAm copolymers and their T_{cp}s. Transitions were narrow and occurred at 40.2, 46.7, 48.8, and 63.9 °C for 20, 30, 40, and 60% copolymer content, respectively.

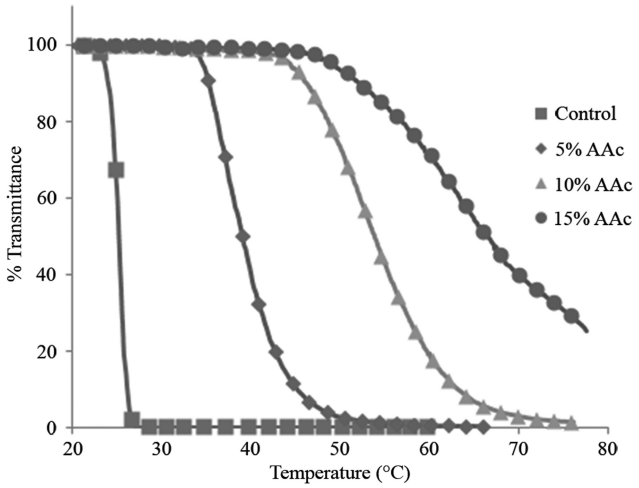

FIGURE 9 pNIPAAm-*co*-AAc copolymers and their T_{cp}s. Transitions were rather broad and occurred at 39.0, 54.0, and 66.4 °C for 5, 10, and 15% copolymer content, respectively.

increased with copolymer content. While the increase in transition range with copolymer content can be explained by the inclusion of more non-pNIPAAm monomers in the polymer chains, the dependence on copolymer type cannot. As these are likely random copolymers, the implication is that the hydrophilicity of the copolymer drastically alters the hydrogen-bonding structure of the surrounding pNIPAAm and thus, its responsiveness. As the transition range is not conserved based on the percentage of copolymer, the sharpness of the transition is not exclusively dependent on the statistical placement of copolymer in the polymer backbone.

We propose that this effect is due to the hydrophobic properties of the comonomers. The methyl pendant groups on DMA can be co-opted into the hydrophobic structures generated by pNIPAAm, yielding a stronger and more definitive response. In fact, it is not until 50% copolymer is incorporated that the range significantly deviates from the control. AAm lacks these pendant groups but is compact, behaving like a void space in terms of hydrophobic side groups, and is therefore unlikely to disrupt the hydrophobic structures significantly. The ability of the pNIPAAm hydrophobic groups to compensate for these voids, however, is strongly dependent on copolymer content. Therefore, as seen in Figure 10, the transition range increases nonlinearly with AAm content. AAc, on the other hand, is charged at neutral pH and strongly hydrogen bonds to multiple water molecules. While it is also compact like AAm, the number of bound water molecules and configuration of these strongly favored bonds disrupts the surrounding hydrophobic system. This disruption inhibits polymer collapse to varying degrees depending on location and number of AAc groups present in a particular chain. A broad transition is therefore observed in these copolymers, even at low AAc content.

CONCLUSIONS

Highly branched pNIPAAm is at once more sensitive and more robust than its linear counterpart. As such, many of the manipulations used in linear systems to change the transition temperature are either less effective or have confounding effects when used in a highly branched system. End-group control, for example, was less effective despite the highly branched system having more end groups than its linear counterpart. Copolymerization, however, was more effective due to the close packing of the system. A racemo diad-inducing agent has the opposite effect due to acceleration in the polymerization, causing meso diad formation instead. Because of these issues, the only way to significantly raise the LCST of highly branched pNIPAAm is to use large amounts of copolymer. Other methods are useful in fine-tuning the transition, but by themselves are not effective enough to induce large changes in the LCST as necessary in applications such as controlled drug delivery.

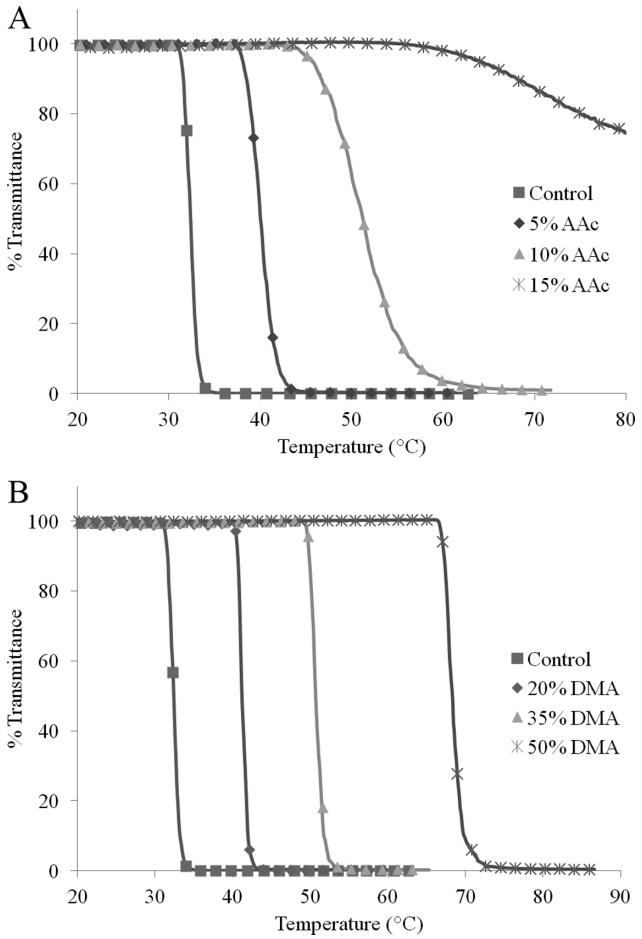

FIGURE 10 (A) Linear pNIPAAm-*co*-AAc copolymers and their T_{cp}s. Transitions occurred at 40.0 and 51.2 °C for 5 and 10% copolymer content, respectively. AAc content (15%) started transitioning at 62 °C but did not complete its transition. (B) Linear pNIPAAm-*co*-DMA copolymers and their T_{cp}s. Transitions occurred at 41.2, 50.6, and 68.3 °C for 5, 10, and 15% copolymer content, respectively.

TABLE 2 pNIPAAm Copolymer Content, Transition Temperature and Range

	Alpha[a]	Feed Ratio (NIPAAm/ Comonomer)	Actual Composition (NIPAAm/Comonomer)	T_{cp} (°C)	Deviation	Range (°C)
pNIPAAm	0.15	100/0	100/0	27.4	26.6–28.1	1.5
5% AAc[b]	0.17	95/5	96/4	39	34.5–48.5	14
10% AAc[b]	0.16	90/10	91/9	53.8	43.5–66.1	22.6
15% AAc[b]	0.13	85/15	83/17	66.6	49.2–80+	30+
20% DMA[c]	0.15	80/20	81/19	33.3	32.7–34.1	1.4
35% DMA[c]	0.04	65/35	64/36	40.9	40.2–41.9	1.7
50% DMA[c]	0.03	50/50	49/51	53.9	52.8–55.2	2.4
100% DMA[c]	0.08	0/100	0/100		No transition	
20% AAm[b]	0.02	80/20	74/26	40.2	38.8–41.3	2.5
30% AAm[b]	NS[d]	70/30	68/32	46.7	44.1–48.6	4.5
40% AAm[b]	NS[d]	60/40	60/40	48.8	45.3–51.5	6.2
60% AAm[b]	NS[d]	40/60	37/63	64.9	59.9–70.7	10.8
pNIPAAm-linear		100/0	100/0	32.4	31.2–33.9	1.7
5% AAc-linear[b]		95/5	95/5	40	37.4–43.4	6
10% AAc-linear[b]		90/10	90/10	51.2	45.0–58.5	13.5
20% DMA-linear[c]		80/20	78/22	41.2	40.4–42.8	2.4
35% DMA-linear[c]		65/35	63/37	50.6	49.7–53.5	3.8
50% DMA-linear[c]		50/50	48/52	68.3	66.7–70.7	4

Copolymer content calculated via ^{1}H NMR. T_{cp} and transition range increase with copolymer content.

[a] Alpha values calculated using GPC with a universal calibration. Linear polymers were analyzed using a linear calibration and model which did not produce alpha values.

[b] NIPAAm content calculated from ^{1}H NMR by dividing the integral of the isopropyl peak (~4 ppm) from the proton-adjusted integral of backbone polymer peaks (~1.2–3.5 ppm).

[c] NIPAAm content calculated from ^{1}H NMR by dividing the integral of the isopropyl peak (~4 ppm) with the sum of the integral of the isopropyl peak and the proton-adjusted integral of the dimethyl peak (~2.8 ppm).

[d] Copolymers with higher amounts of AAm were not soluble (NS) in THF for this analysis.

ACKNOWLEDGMENTS

The authors thank Leslie Gelbaum for assistance with NMR, F. Joseph Schork for helpful discussions, and the Georgia Tech Center for Drug Design, Development, and Delivery (CD4) Graduate Assistance in Areas of National Need (GAANN) Fellowship for funding.

REFERENCES AND NOTES

1 R. T. A. Mayadunne, J. Jeffery, G. Moad, E. Rizzardo, *Macromolecules* **2003,** *36*, 1505–1513.

2 L. Barner, T. P. Davis, M. H. Stenzel, C. Barner-Kowollik, *Macromol. Rapid Commun.* **2007,** *28*, 539–559.

3 C. J. Hawker, R. Lee, J. M. J. Fréchet, *J. Am. Chem. Soc.* **1991,** *113*, 4583–4588.

4 M. Ballico, S. Drioli, G. M. Bonora, *Eur. J. Org. Chem.* **2005,** *2005*, 2064–2073.

5 J.-J. Yan, C.-Y. Hong, Y.-Z. You, *Macromolecules* **2011,** *44*, 1247–1251.

6 Z. Wu, H. Liang, J. Lu, *Macromolecules* **2010,** *43*, 5699–5705.

7 S. Carter, S. Rimmer, R. Rutkaite, L. Swanson, J. P. A. Fairclough, A. Sturdy, M. Webb, *Biomacromolecules* **2006,** *7*, 1124–1130.

8 X. Yang, J. J. Grailer, I. J. Rowland, A. Javadi, S. A. Hurley, V. Z. Matson, D. A. Steeber, S. Gong, *ACS Nano* **2010,** *4*, 6805–6817.

9 Y. Liu, K. Li, B. Liu, S.-S. Feng, *Biomaterials* **2010,** *31*, 9145–9155.

10 S. Hopkins, S. Carter, L. Swanson, S. MacNeil, S. Rimmer, *J. Mater. Chem.* **2007,** *17*, 4022–4027.

11 T. Higashihara, Y. Segawa, W. Sinananwanich, M. Ueda, *Polym. J.* **2012,** *44*, 14–29.

12 S. Carter, S. Rimmer, A. Sturdy, M. Webb, *Macromol. Biosci.* **2005,** *5*, 373–378.

13 S. Carter, B. Hunt, S. Rimmer, *Macromolecules* **2005,** *38*, 4595–4603.

14 K. Matyjaszewski, S. G. Gaynor, A. Kulfan, M. Podwika, *Macromolecules* **1997,** *30*, 5192–5194.

15 S. G. Gaynor, S. Edelman, K. Matyjaszewski, *Macromolecules* **1996,** *29*, 1079–1081.

16 B. Liu, A. Kazlauciunas, J. T. Guthrie, S. Perrier, *Macromolecules* **2005,** *38*, 2131–2136.

17 A. P. Vogt, B. S. Sumerlin, *Macromolecules* **2008,** *41*, 7368–7373.

18 A. Zargar, K. Chang, L. J. Taite, F. J. Schork, *Macromol. React. Eng.* **2011,** *5*, 373–384.

19 T. Shanmugam, A. Raghavan, A. S. Nasar, *J. Macromol. Sci. Pure Appl. Chem.* **2006,** *43*, 1387–1397.

20 Y. Segawa, T. Higashihara, M. Ueda, *J. Am. Chem. Soc.* **2010,** *132*, 11000–11001.

21 Z. Guan, P. M. Cotts, E. F. McCord, S. J. McLain, *Science* **1999,** *283*, 2059–2062.

22 A. P. Vogt, S. R. Gondi, B. S. Sumerlin, *Aust. J. Chem.* **2007,** *60*, 396–399.

23 J. Chiefari, Y. K. Chong, F. Ercole, J. Krstina, J. Jeffery, T. P. T. Le, R. T. A. Mayadunne, G. F. Meijs, *Macromolecules* **1998,** *31*, 5559–5562.

24 K. Chang, Z. T. Dicke, L. J. Taite, *J. Polym. Sci. Part A: Polym. Chem.* **2012,** *50*, 976–985.

25 G. L. Ellman, *Arch. Biochem. Biophys.* **1959,** *82*, 70–77.

26 T. Hirano, T. Kamikubo, Y. Fujioka, T. Sato, *Eur. Polym. J.* **2008,** *44*, 1053–1059.

27 T. Hirano, T. Kamikubo, Y. Okumura, T. Sato, *Polymer* **2007,** *48*, 4921–4925.

28 T. Hirano, Y. Okumura, H. Kitajima, M. Seno, T. Sato, *J. Polym. Sci. Part A: Polym. Chem.* **2006,** *44*, 4450–4460.

29 M. Koyama, T. Hirano, K. Ohno, Y. Katsumoto, *J. Phys. Chem. B* **2008,** *112*, 10854–10860.

30 B. Ray, Y. Isobe, K. Morioka, S. Habaue, Y. Okamoto, M. Kamigaito, M. Sawamoto, *Macromolecules* **2003,** *36*, 543–545.

31 T. Hirano, H. Miki, M. Seno, T. Sato, *Polymer* **2005,** *46*, 3693–3699.

32 D. Hölter, A. Burgath, H. Frey, *Acta Polym.* **1997,** *48*, 30–35.

33 W. Tao, L. Yan, *J. Appl. Polym. Sci.* **2010,** *118*, 3391–3399.

34 H. Mori, D. C. Seng, H. Lechner, M. Zhang, A. H. E. Müller, *Macromolecules* **2002,** *35*, 9270–9281.

35 D. S. Thompson, L. J. Markoski, J. S. Moore, *Macromolecules* **2000,** *33*, 6412–6415.

36 C.-H. Ho, S.-A. Chen, M. D. Amiridis, J. W. V. Zee, *J. Polym. Sci. Part A: Polym. Chem.* **1997,** *35*, 2907–2915.

37 T. Hirano, H. Kitajima, M. Seno, T. Sato, *Polymer* **2006,** *47*, 539–546.

38 B. Ray, Y. Okamoto, M. Kamigaito, M. Sawamoto, K.-I. Seno, S. Kanaoka, S. Aoshima, *Polym. J.* **2005,** *37*, 234–237.

39 Y. Xia, N. A. D. Burke, H. D. H. Stöver, *Macromolecules* **2006,** *39*, 2275–2283.

40 B. S. Sumerlin, A. P. Vogt, *Macromolecules* **2010,** *43*, 1–13.

41 G.-Z. Li, R. K. Randev, A. H. Soeriyadi, G. Rees, C. Boyer, T. P. Davis, R. Becer, D. M. Haddleton, *Polym. Chem.* **2010,** *1*, 1196–1204.

42 X.-P. Qiu, F. M. Winnik, *Macromol. Rapid Commun.* **2006,** *27*, 1648–1653.

43 J. Mazzolini, O. Boyron, V. Monteil, F. D'Agosto, C. Boisson, G. C. Sanders, J. P. A. Heuts, R. Duchateau, D. Gigmes, D. Bertin, *Polym. Chem.* **2012,** *3*, 2383–2392.

44 Z. Li, Y.-H. Kim, H. S. Min, C.-K. Han, K. M. Huh, *Macromolecular Research* **2010,** *18*, 618–621.

45 G. Ru, J. Feng, *J. Polym. Sci. Part B: Polym. Phys.* **2011,** *49*, 749–755.

46 J. A. Orlicki, N. O. Viernes, J. S. Moore, *Langmuir* **2002,** *18*, 9990–9995.

47 H. Feil, Y. H. Bae, J. Feijen, S. W. Kim, *Macromolecules* **1993,** *26*, 2496–2500.